# Ultrafast Spin and Magnetization Dynamics: Coupling of Spin to Electronic and Lattice Degrees of Freedom

**Evan Anderson**
*Ultrafast Optics. Phys 7660*
*evan.j.anderson@colorado.edu*

## 1. Introduction

For a long period of time it was thought that the best way to influence the the magnetic order of was with an induced magnetic field, typically by running a current through a wire. In the 20th and 21st century however, optical manipulation of magnetic order has become mainstream. In fact, ultrafast laser pulses have shown that manipulation can occur on the femtosecond timescale. It was thought, due to weak spin-orbit coupling that picosecond or faster demganetization could not occure. However this has since been proven and a primary question has become how do spin, electronic and lattice degrees of freedom interact on such timescales and what is the mechanism behind ultrafast demagnetization.

In this paper I will begin by discussing potential applications and challenges faced with ultrafast optical manipulation of magnetic order. I will then give a broad overview of experimental techniques in manipulating magnetic order with ultrafast laser pulses. Following that, the seminal experiment by Beurepaire et al. which showed sub-picosecond demagnetization will be discussed. After setting the scene, I will discuss the three temperature model commonly used to relate spin, electronic and lattice degrees of freedom and begin to explore their relationships. Next I will discuss more current research which continues to explore the relationships devised in the three temperature model and expand it even further. I will finally conclude with a perspective and brief overview of the work.

## 2. Applications and Challenges

### *2.1. Applications*

While doing science for the sake of discovery of new phenomena has merit in its own right, traditionally it is not funded very well. Fortunately in the case of ultrafast manipulation of magnetic order, there are lucrative applications. The first application is increased read/write speed of magnetic storage. Currently, commercial magnetic media has a read/write speed on the order of nanoseconds and a theoretical limit in the many of picosecond regime [1]. It should also be noted that magnetic media has not followed the traditional Moore's law of computing and thus not kept up with the processor speed of today's computers. Ultrafast optical pulses however have been shown to be able to manipulate the magnetic order on the femtosecond time scale, a $10^6$x speedup from today's speeds. Other areas and of spintronics such as magnetic sensors or magnetic random access memory can also benefit from studying these ultrafast interactions. Figure 1 shows relavent times scales on which a laser pulse vs magnetic field and alludes to possible mechanisms which could be responsible for the sub picosecond manipulation. [2]

### *2.2. Challenges*

Studying ultrafast optical interactions with magnetic order has proven challenging. There are a few reasons for this, the first of which is that ultrafast pulses put magnetic mediums in highly nonequilibrium states. This becomes troublesome as one can no longer only consider the sum of the individual magnetic moments (i.e. the macro-spin approximation breaks down) but must take them into consideration individually. As a result of the large amount of engery deposited into a system, and subsequent breakdown of the macro-spin approximation, the theory of magnetic phenomena with respect to thermodynamics is no longer valid.

Additionally, a laser pulse on a magnetic medium has three types of effects: thermal, nonthermal and nonthermal optomagnetic. It should be noted though, in practice, there are always thermal effects. The thermal effects, which will be a main focus of the paper deal with energy from the laser pulse being deposited into the lattice and electron systems. It cannot be effectively be deposited into the spin system as electric-dipole approximation spin-flip transitions are forbidden. At higher approximations the interaction is extremely weak. The equilibrium processes ultimately determines

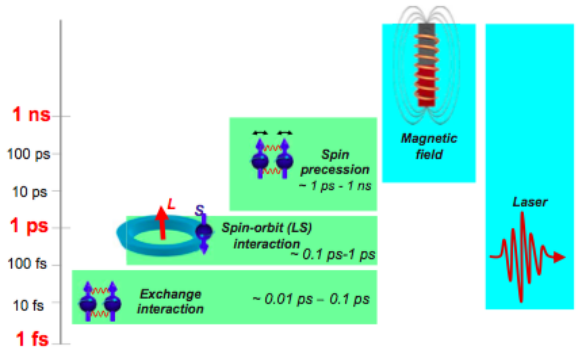


Fig. 1. Timescales of magnetic properties and the relative time scales between generating a magnetic field and laser pulse. [2]

the time scale of the magnetic order manipulation. These include electron-electron, electron-phonon, and electron-spin interactions. The times scales on which some of these occurcan be seen in figure 1.

Nonthermal photomagnetic effects involve the absorption of energy from photons by electronic states which influence magnetic parameters. These are typically longer than those of the thermal effects

Third, there are the nonthermal optomagnetic effects which use a optically coherent stimulated Raman scattering mechanism. These effects only interact on spin-orbit coupling and have a lifetime of optical coherence, typically 100-200 fs. [2]

## 3. Experimental Techniques and Foundations

### *3.1. Experimental Techniques*

In almost all ultrafast optical manipulation of magnetic order experiments, some sort of pump-probe technique is used with the length of the probe pulse ultimately defines the temporal resolution of the results. Experimental techniques then differ by which spectral range is chosen as they have different sensitivity to the orbital and spin degrees of freedom.

The infrared range can be used as an indirect probe for specific phase transitions in magnetic material. This is due to the free electrons having a very large response to photons with infrared energies. This Drude response also gives incite to the conductivity.

In the optical range, for a magnetically ordered medium with static magnetization $\mathbf{M}(0)$ or anti-ferromagnetic vector $\mathbf{l}(0)$, one can consider the thermodynamic potential $\phi$. With a laser producing a field $\mathbf{E}(\mathrm{w})$, $\phi$ can be written as:

$$\begin{aligned}\phi = \chi_{ij}E_i(w)^*E_j(w) + \alpha_{ijk}E_i(w)^*E_j(w)M(0)_k + \beta_{ijk}E_i(w)^*E_j(w)l(0)_k \\ + \chi_{ijk}E_i(2w)^*E_j(w)E_k(w) + \alpha_{ijkl}E_i(2w)^*E_j(w)E_k(w)M(0)_l + \beta_{ijkl}E_i(w)^*E_j(w)E_k(w)l(0)_l \quad (1)\end{aligned}$$

Here, $\chi$, $\alpha$, and $\beta$ are tensors that define optical properties including magneto-optical an anti-ferromagnetic susceptibility. It can be seen then one can find both the magnetization $\mathbf{M}(0)$ and anti-ferromagnetic vector $\mathbf{l}(0)$ from the linear terms alone.

Additionally, the polarization $\mathbf{P}(\mathrm{w})$ gives a definition of the linear optical response of a medium to a field $\mathbf{E}(\mathrm{w})$. This should then give a polarization $\mathbf{P}^{(m)}$ proportional to magnetization. Because of this, the light reflected from a magnetic medium can become rotated and the rotation recorded. This is called the magneto-optical Kerr effect (MOKE). This rotation can thus be used as a probe for the current magnetic state of a given medium.

Unlike the optical regime with MOKE, the ultraviolet regime allows for direct as opposed to indirect measurement of the average spin polarization. This is because the energy of the pulse is typically higher than the work function of the magnetic medium thus releasing an electron from the surface. The average spin polarization can then be measured directly from a group of electrons. Unfortunately, in the UV spectrum, one must have a high quality surface, and conductivity which limits what materials can be used in this regime.

Finally, the X-ray regime provides very similar insights as the optical, namely the ability to measure the orientation of the magnetization and anti-ferromagnetic vector. The orientation is then used as an indirect probe. This is done using a technique called X-ray magnetic circular dichroism (XMCD) which compares spectra taken by left and right circularly polarized light. XMCD has an added benefit that the optical range does not - due to the narrow transitions and well-defined energies, XMCD can be used to associate demagnetization to elemental and chemical specificity.

### *3.2. Foundations*

In 1991, it was assumed that the spin-lattice relaxation times of metallic ferromagnets was in the on the range of 100 $\pm$ 80 ps. This was observed by Vaterlaus, Beutler and Meier who used 60ps - 10ns pulses to measure the relaxation time [3]. As can be seen, the pulses were on the same order as that of the measured relaxation time, as a result, this meant that portions of the system were always in equilibrium. It was not until 1994 that optical demagnetization was observed on even faster timescales.

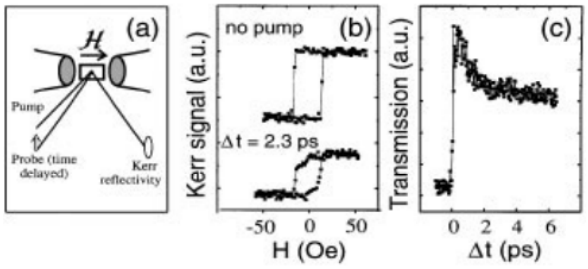


Fig. 2. (a) Pump-probe setup for the dynamic longitudinal Kerr effect. (b) Hysterisis loops with and without a pump pulse. (c) Transient transmitivity over a 6ps time scale. [4]

Beurepaire et al. used much faster pulses that those previously. They used 60fs pulses incident on Ni film in their experimental setup. Figure 2a shows Beurepaire et al.'s pump-probe setup allowing for measurement of transient transmission or reflectivity from the dynamic longitudal Kerr effect. The hysteresis loop seen in figure 2b shows the first indication of demagnetization. When there is no pump pulse, a normal loop for a magnet is seen. However, when the pump is turned on, a dip seen at 0 H is seen which is indicative of demagnetization. In figure 2c, a typical transient transmission curve is seen while noting a majority of the dip occurs within the 2 ps time scale.

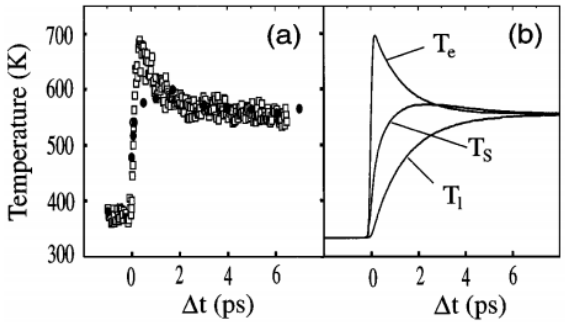


Fig. 3. (a) Experimental spin (black circles) and electron temeperatures (open squares) estimates. (b) Spin ($T_s$), electron ($T_e$) and lattice ($T_l$) temperatures calculated from the three temperature model [4]

Beurepaire et al. was also able to study the thermalization process and deduce and electron temperature $T_e$ by doing pump-probe transmission measurements without the presence of a magnetic field. This is done by assuming that the temperature $T_e$ is proportional to the transmittance seen in figure 2c. The calculated experimental temperature $T_e$ in figure 3a (open squares) and is plotted alongside the spin temperature $T_s$ (black circles) which was calculated from the observed normalized remanence. Figure 3b shows the calculated temperatures using the three temperature model

Beurepaire et al. developed. It is the basis of the thermal interactions between electronic, lattice and spin degrees of freedom as discussed in the next section.

## 4. Three Temperature Model

As mentioned in the previous section, Beurepaire et al. developed a three temperature model to describe the interactions between the electronic, lattice, and spin degrees of freedom. It takes the form of three coupled differential equations:

$$C_e(T_e)\frac{dT_e}{dt} = G_{el}(T_e - T_l) - G_{es}(T_e - T_s) + P(t),$$

$$C_s(T_s)\frac{dT_s}{dt} = G_{es}(T_s - T_e) - G_{sl}(T_s - T_l),$$

$$C_l(T_l)\frac{dT_l}{dt} = G_{el}(T_e - T_l) - G_{sl}(T_s - T_l)$$

Here, $G_{ij}$ refers to the *i*-*j* interaction constants (e.g. $G_{es}$ is the electron-spin interaction strength), $T_i$ is the temperature of a given system and $C_i$ is the specific heat for each system within the given material. $P(t)$ is only seen in the electronic equation and represents the coupling of the laser pulse into the overeall system. This relationship can be pictorially seen in figure 4. [4]

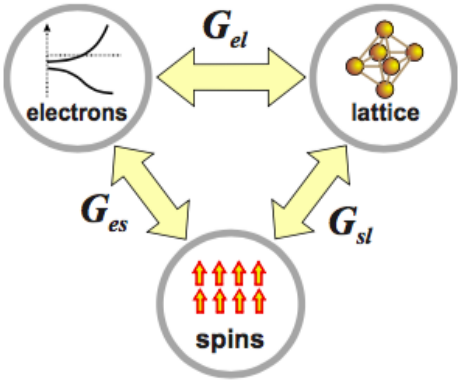


Fig. 4. Pictoral representation of the three temperature model for electronic, lattice and spin interactions. [2]

With respect to heat capacities, it is typical for $C_e$ to be a few orders of magnitude smaller than $C_l$. This implies that $T_e$ can reach very high temperatures after the initial pulse while the lattice itself has little to no response even after the systems have come into equilibrium. To illustrate the relationship, an example scenario is described:

1. A laser pulse hits the sample and creates hot electrons in 1 fs
2. The electrons begin to equilibrate at high $T_e$ via electron-electron interactions on a time scale of 10-100 fs as seen in figure 1
3. The electronic excitations begin to decay and heat up the lattice ($T_l$) via phonon cascades. This occurs on the 1-10 ps time scale depending on the material as can be seen in figure 3b.

The big question however is what mechanism drives the spin relaxation. This relaxation must come in the form of angular momentum transfer as demagnetization occurs. The only place for the angular momentum to go is another reservoir be it lattice or electronic. Both reservoirs should be able to absorb the angular momentum, however it was initially thought that the interaction coefficients between the spin and other two reservoirs were much weaker than they are, leading to a relaxation time on the order of 300 ps in Ni, which is clearly much larger than the 1 and 2 ps observed by Beurepaire et al..

There are three main ideas behind spin-orbit coupling where the angular momentum of the spin system is transferred into the electronic system. It should first be noted that the spin-orbit coupling is a prime candidate to describe the ultrafast demagnetization as a relaxtion time of 20fs can be achieved in metals. The three mechanisms are the Elliott-Yafet mechanism, inelastic electron-spin-wave scattering events and a Stoner excitation.

The Elliott-Yafet mechanism can cause spin relaxation because the conduction band electron states are not technically pure spin states. This means that when an electron scatters to another state in the conduction band it has a chance to couple to a new spin state causing spin relaxation.

Stoner excitations are electron-hole pair excitations. These electron-hole pairs however are highly dependent on the band structure, the electron-electron interactions and itinerant-electron systems in a metal typically lead to band with spin-up and spin-down electrons. A Stoner excitation is then an electron-hole pair with a hole in one band and the electron in the other. An electron thus may be removed from one band, do a spin-flip and move to another, reversing the Stoner excitation vector. It should be noted that Stoner excitations typically are only observed at relatively high energies as at low energies, the configuration of the electronic bands do not necessarily arrange in a spin-up and spin-down configuration. The exact mechanism be it spin-lattice or one of the spin-orbit coupling mechanisms described is still actively researched and debated. [2]

It is also quite common to see a two step demagnetization process. This process involves the non-equilibrium state corresponding to a demagnetization on sub-picosecond time scales and later a secondary demagnetization in an equilibrium state on the 10s - 100s picosecond time scales. Until recently it was thought that it was a direct result of spin-orbit coupling and spin-lattice coupling via spin-orbit interactions. Recent research however suggests otherwise. [5]

### *4.1. Current Research*

In 2014, Eschenlohr et al. devised a clever way to discover which reservoir was responsible for optical ultrafast demagnetization. They did this by measuring effects on various $Gd_{x-1}Tb_x$ alloys.

To understand how one can determine the spin-lattice mechanism, one must first understand how the electron-phonon coupling in the alloy works. In Tb, a strong spin-lattice coupling can be deduced from the anisotropic orbital configuration due to the $4f^8$ electron configuration creating and orbital moment of $L = 3$. In Gd, the configuration is $4f^7$ leading to an orbital moment of $L = 0$ and a weaker spin-lattice coupling. In both cases, the $4f$ moments are coupled to the lattice through the $5d$ electrons as well. However, in the case of Gd, this is the primary coupling mechanism whereas Tb also couples directly through the $4f$ electrons. These couplings can be see in figure 5b. It can be seen then with different values of Tb and Gd, the alloy should exhibit different spin-lattice coupling strengths.

There were two main experiments preformed. The first time resolved MOKE and the second was time resolved XMCD. As mentioned earlier, MOKE allows for an indirect probe of the magnetization and subsequently the concentration dependent magnetization dynamics of the $5d$ electrons. This setup can be observed in figure 5a where a pump pulse excites the $5d$ electrons and probed with MOKE of similar energy. The second experiment used XMCD in order to properly separate the dynamics of Tb and Gd to confirm relative strengths of the spin-lattice coupling. This setup can also be seen in figure 5a where XMCD excited the $3d_{5/2}$ electrons to the unoccupied $4f$ states.

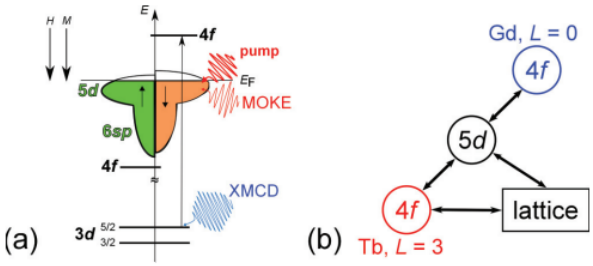


Fig. 5. (a) Electronic density of states for Gd and Tb and which energy states are probed with MOKE and pumped with XMCD. (b) Configuration of coupling of the $4f$ and $5d$ moments to the lattice alloy. [5]

In the MOKE setup, a Ti:sapphire oscillator was used with a wavelength of 790 nm, generating 35 fs pulses at 1.52 MHz. The Tb and Gd content the $Gd_{x-1}Tb_x$ alloy was varied from $x = 0$ to $x = 0.7$. Figure 6 shows the transient Kerr

rotation with respect to the pump-probe delay. It is clear that increasing Tb content in the alloy greatly effects the demagnetization curves. This is explained by the static temperature dependence of magnetization. The Curie temperature $T_c$, or temperature at which a material loses its magnetization, is lower for Tb than Gd, so it would make sense that decreasing $T_c$ of the alloy while keeping the alloy's temperature the same would induce increased demagnetization. Another key feature of the MOKE results is that there is two clear demagnetization events occurring for each $x$. The first drop in magnetization has a time constant ($\tau_1$) on the 1-2 ps range for all alloys whereas the second drop occurs on a much larger time scale with time constants ($\tau_2$) ranging from 16 to 100 ps. $\tau_2$ is negatively correlated with $x$, that is, as Tb increases in the alloy, $\tau_2$ decreases, ultimately reaching maximal demagnetization faster. The MOKE results however could not explain the reason for the accelerated demagnetization as to whether it was due to the increase in Tb as $x$ increased, or the decreasing Gd.

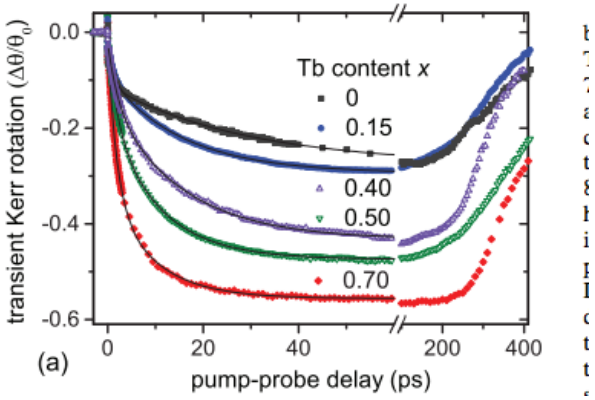


Fig. 6. MOKE response vs pump-probe delay. Two demagnetization events can be seen, one on the 1-2ps timescale and another in 10-50ps for varying Gd and Tb amounts. [5]

While MOKE can not determine the mechanism behind the accelerated demagnetization for increased $x$, XMCD was the perfect candidate as it can separate the dynamics of the two elements. The samples were excited using a 50 fs pulse with 780 nm wavelength. X-Ray probe pulses were generated using a BESSY II femtoslicing source with a duration of 100 fs at 6 kHz. The combination of this setup allowed for 130 fs time resolution. The results of the XMCD measurements can be seen in figure 7. As expected, a clear distinction between the demagnetization of the two elements can be seen. It can also be seen, similar to the MOKE results that the demagnetization process happens in two steps. The first process occurs in under a picosecond and is half the total demagnetization. The second demagnetization effect occurs on a 20 ps time scale. It is also important to note that during the first drop, decrease in magnetization of both Tb and Gd, was the same. The second drop however saw a larger demagnetization in Tb and Gd.

The first demagnetization had time constants $0.89 \pm 0.29$ ps and $1.03 \pm 0.25$ ps for Gd and Tb respectively in a $Gd_{0.6}Tb_{0.4}$ alloy. In previous work done by Wietstruk et al. it was found that this time constant was $0.76 \pm 0.25$ ps for pure Gd and $0.74 \pm 0.25$ ps for pure Tb [6]. In both cases, the alloy Gd and Tb time constants fall within the error bars of the pure versions. However, in the second demagnetization step a time constant of $5.3 \pm 2.3$ ps was observed for the alloy for both Tb and Gd. Time constants for pure Tb and Gd were much different however, $8 \pm 3$ ps and $40 \pm 10$ ps respectively. This suggests that it is a direct result of the spin-lattice coupling previously mentioned and seen in figure 5b.

In both the MOKE and XMCD results, two demagnetization processes were observed. In the MOKE setup, an overall increased demagnetization with increased Tb occured. This was explained by a decrease in $T_c$. In the second, longer demagnetization process, the varying time constants was explained by the strength of the spin-lattice coupling of relative Tb and Gd. This was also confirmed by the XMCD results. This unequivocally shows that the second process is due to spin-lattice coupling and is explained by the orbital antisotropy of the $4f$ shell.

The sub-picosecond time scale of the first demagnetization step corresponds to a highly non-equilibrium state. This, coupled with the facts that the amount of demagnetization and time constants remained the same in both the MOKE and XMCD results suggest the demagnetization starting with the excited $5d$ electrons. In the three temperature model discussed earlier, electron-lattice spin-flip via the Elliott-Yafet effect was used to explain sub-picosecond demagnetization. Two step processes in the model however is only suppose to occur when the spin-orbit coupling itself is weak.

However, both Tb and Gd have relatively strong spin-orbit coupling. Additionally, the spin-lattice coupling via spin-orbit interactions of Gd and Tb have two very different strengths, implying that there is more to the three temperature model which causes a two step process. In particular, direct spin-lattice coupling of the $4f$ moments in this case need to be considered. [5]

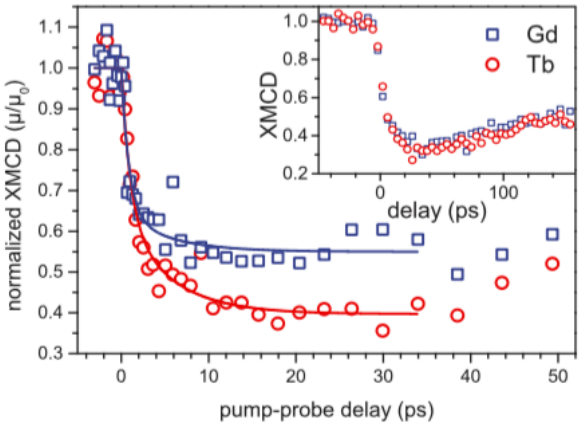


Fig. 7. Results from XMCD measurements on a $Gd_{0.6}Tb_{0.4}$ alloy with 130 fs resolution. The inset shows results using 10 ps x-ray pulses. [5]

## 5. Summary and Perspective

Optically induced ultrafast manipulation of magnetic order has become a very interesting field over the last two decades with the discovery of sub picosecond demagnetization. This discovery has many potential applications in spintronics and magnetic media. The field itself is not without its challenges however, many of the traditional theories and approximations break down and there are many effects that need to be taken into consideration. Experimentally, observing the manipulation of magnetic order almost always uses some combination of pump and probe technique. The two spectral regimes to run these experiments that have emerged the most useful are the optical and x-ray. In the optical regime, one observers MOKE, in which polarized light becomes rotated based on the magentization of a medium and is thus an indirect probe of the magnetization. Similarly XMCD is also an indirect probe but gives additional information such as being able to separate elemental or chemical dynamics due to well-defined energy levels. Other regimes such as UV and infrared may also be used but are highly dependent on the medium itself.

The seminal work by Beurepaire et al. first introduced the world to sub picosecond demagnetization. Beurepaire et al. thus also developed the three temperature model to help describe their results. This model involves three coupled differential equations to relate spin, electronic and lattice degrees of freedom. Prior to this, all demagnetization effects had been seen in an semi-equilibrium or equilibrium state and thought that the spin-orbit and spin-lattice coupling was too weak to produce such fast demagnetization. There are now mechanisms and theories which support stronger couplings such as the the Elliott-Yafet mechanism which works off the basis of electron scattering in the conduction band coupling to new spin states.

Current research continues to explore the interactions of the three temperature model such as the work done in 2014 by Eschenlohr et al.. In their experiment, they were able to use MOKE and XMCD to deduce that in two step demagnetization processes, the first step is due to spin-orbit coupling, but cannot be successfully described by the the Elliott-Yafet mechanism. Eschenlohr et al. were also able to show second step is a result of spin-lattice coupling is explained by the orbital antisotropy of the $4f$ shell and not via spin-orbit interactions as originally explained in the three temperature model. Thus the authors suggest that further examination of direct spin-lattice coupling needs to be considered.

It is clear then that ultrafast spin and magnetization dynamics is still not fully understood. It is interesting to see how a single experiment introducing not only sub-picosecond demagnetization but a model to describe it has been so accurate for 20 years. However, it is also very interesting to see the how evolution of the field has come about and how the three temperature is continually being slightly modified when new discoveries are made. I look forward to learning

about the true underlying mechanisms and relationships of these systems moving forward.

## References


1. C.H. Back, and D. Pescia, D., "Speed Limit Ahead", Nature **428**, 808-809 (2004).
2. A. Kirilyuk, A.V. Kimel, and T. Rasing, "Ultrafast optical manipulation of magnetic order" Rev. of Mod. Phys. **82**, 2744-2784 (2010).
3. A. Vaterlaus, T. Beutler, and F. Meier, "Different spin and lattice temperatures observed by spinpolarized photoemission with picosecond laser pulses", J. Appl. Phys. **67**, 5661 (1990).
4. E. Beaurepaire, J.C Merle, A. Daunois, and J. Y. Bigot, "Ultrafast Spin Dynamics in Ferromagnetic Nickel", Phys. Rev. Lett. **76**, 4250 (1996).
5. A. Eschenlohr, M. Sultan, A. Melnikov, N. Bergeard, J. Wieczorek, T. Kachel, C. Stamm, and U. Bovensiepen, "Role of spin-lattice coupling in the ultrafast demagnetization of $Gd_{1x}Tb_x$ alloys", Phy. Rev. B **89** 214423 (2014).
6. M. Wietstruk, A. Melnikov, C. Stamm, T. Kachel, N. Pontius, M. Sultan, C. Gahl, M. Weinelt, H. A. Durr, and U. Bovensiepen, "Hot-Electron-Driven Enhancement of Spin-Lattice Coupling in Gd and Tb $4f$ Ferromagnets Observed by Femtosecond X-Ray Magnetic Circular Dichroism" , Phys. Rev. Lett. **106**, 127401 (2011).